

Conformations of (1→4)-linked α -D-galacturono-di- and -tri-saccharides in solution analysed by n.m.r. measurements and theoretical calculations

Miloš Hricovíni^{*†}, Slavomír Bystrický, and Anna Malovíková

Institute of Chemistry, Slovak Academy of Sciences, 842 38 Bratislava (Czechoslovakia)

(Received December 17th, 1990; accepted for publication March 28th, 1991)

ABSTRACT

The conformations of the (1→4)-linked α -D-galacturono-di- (**1**) and -tri-saccharide (**2**) in aqueous solutions have been analysed by n.m.r. spectroscopy and MM2CARB calculations. The $^3J_{\text{C,H}}$ and n.O.e. values did not change with temperature and were comparable for **1** and **2**. Four energy regions were found on the relaxed (ϕ , ψ) map for **1** computed by the MM2CARB method. Theoretical n.O.e. values, based on the geometry and the abundance of the most populated conformer, accorded with experimental values. The magnitudes of ϕ^{H} and ψ^{H} for the glycosidic bond suggest that a right-handed three-fold helical arrangement can be formed by pectic acid oligosaccharides in solution.

INTRODUCTION

Pectin occurs in the cell wall of higher plants and is mainly a (1→4)-linked α -D-galacturonan; its conformation is sensitive to the counter-ions present in solution. Although the conformation induced by association with Ca^{2+} is well understood^{1,2}, those in the presence of monovalent ions and in the acidic form are less clear.

There are contradictions in the literature. The first diffraction studies suggested two-fold³ or three-fold left-handed helical structures for pectic acid⁴. However, model-building computations showed these structures to be different⁵. Simple potential-function calculations⁶ also did not give clear evidence of the structure. More detailed fibre diffraction analyses showed that both sodium pectate and pectic acid have similar three-fold helical structures⁷. Calorimetric measurements of the pH-dependence of the enthalpy of dissociation showed that the anomalous bell-shaped curve⁸ was due to conformational transition. Different conformations were also suggested⁹ on the basis of the differences in c.d. spectra of pectic acid neutralised with calcium or sodium hydroxide. A new method for probing conformation, based on the enantioselective interaction of polyions, showed that D-galacturonan tends to form a right-handed helical structure¹⁰. We have approached the problem by conformational analysis of model compounds, namely, on the basis of n.m.r. data and theoretical calculations for the (1→4)-linked α -D-galacturono-di- (**1**) and -tri-saccharide (**2**).

^{*}To whom correspondence should be addressed.

[†] Present address: Department of Medical Genetics, University of Toronto, Toronto M5S 1A8, Canada.

EXPERIMENTAL

The di- (**1**) and tri-saccharide (**2**), prepared as described^{11,12}, have been characterised fully. The ¹H- (300.13 MHz) and ¹³C-n.m.r. spectra (75.45 MHz) were obtained on 0.1M solutions of **1** and **2** with a Bruker AM-300 spectrometer at 25° and 50°. The chemical shifts were referenced to internal acetone (¹H, 2.225 p.p.m.; and ¹³C, 30.0 p.p.m.).

Homonuclear *J*-resolved experiments were used to determine the *J*_{H,H} values; 128 f.i.d.s were collected, giving a digital resolution of 0.1 Hz/point in the F1 domain. The ³*J*_{C,H} values across the glycosidic bond were measured by modified 2D semiselective INEPT^{13,14}. Soft rectangular pulses with an amplitude $\gamma B_2/2\phi = 20$ Hz were used for the semiselective excitation of the protons. Data matrices were 2K × 64W and typically 64 transients were accumulated in each of 64 f.i.d.s. Selected traces were zero-filled to give a final digital resolution of 0.15 Hz/point. An appropriate weighted function (shifted sine bell in the F2 domain, Gaussian in the F1 domain) was used prior to Fourier transformation.

Experimental n.O.e. values were determined by difference spectroscopy¹⁵ where protons associated with the multiplet were irradiated 50–100-fold with a soft pulse of duration 200–300 ms, using a series of frequency lists to define multiple irradiation points. The total time of irradiation for each multiplet was 10–11 s and the acquisition time was 7 s. Zero filling to give a final resolution of 0.05 Hz was used before Fourier transformation. In order to obtain good thermal equilibrium, each sample was stored 2–3 h at each temperature before measurement in the spectrometer. Two dummy scans preceded each of 128 accumulated transitions.

For **1** and **2**, the torsional angles ϕ^H and ψ^H are defined as H-1'-C-1'-O-1'-C-4 and H-4-C-4-O-1'-C-1', respectively. The calculations of the energies of the conformations were performed by mapping all conformational space in steps of 30° for both ϕ and ψ . The MM2CARB program, which is a version of the force-field program¹⁶ with modified acetal segment parameters¹⁷, was used. The program enabled optimisation of all internal co-ordinates except an arbitrary set of ϕ, ψ angles. The starting geometry was taken from the calculated standard geometry for hexopyranoses¹⁸. Torsion parameters for the carbonyl group were not specially modified for the saccharide moiety. The final geometries of the four lowest energy minima were obtained by further optimisation of ϕ and ψ . The calculated structures represent a molecule in the isolated state. In order to express a solvent effect, a continuum-model approximation¹⁹ was used. Theoretical n.O.e. values were calculated on the basis of the geometry of the major conformer. Three-spin effects were not evaluated.

RESULTS AND DISCUSSION

The chemical shifts of the ¹H resonances and the *J* values for solutions of **1** and **2** in D₂O at 25° are shown in Table I. Compared to the data for the Na⁺ and Ca²⁺ forms²⁰, the chemical shifts and *J* values are not markedly different and varied within 0.1 p.p.m.

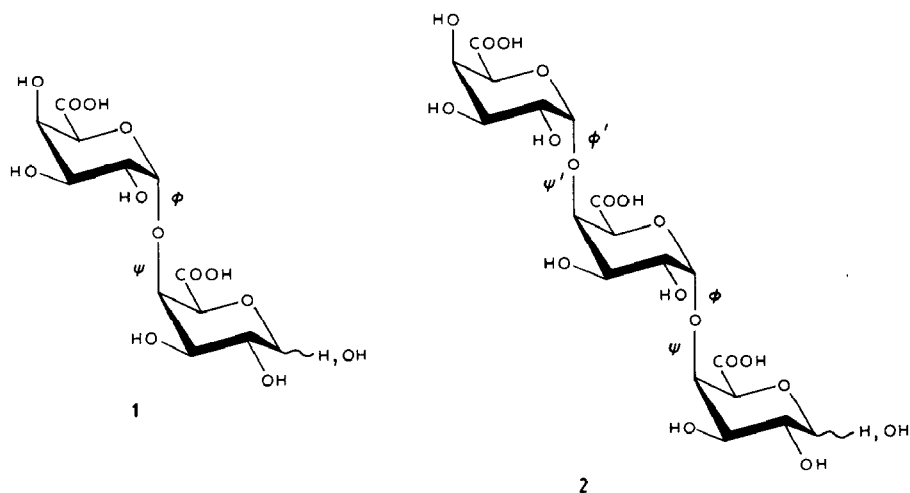


TABLE I

$^1\text{H-N.m.r.}$ data (δ in p.p.m., J in Hz) for solutions of **1** and **2**^a in D_2O at 25° (referenced to internal acetone, 2.225 p.p.m.)

	α	β			
Compound 1					
H-1	5.39	4.69	H-1'	5.13	
H-2	3.87	3.55	H-2'	3.78	
H-3	4.08	3.81	H-3'	3.99	
H-4	4.49	4.42	H-4'	4.37	
H-5	4.68	4.35	H-5'	5.08	
$J_{1,2}$	3.8	7.7	$J_{1',2'}$	4.0	
$J_{2,3}$	11.0	10.5	$J_{2',3'}$	10.8	
$J_{3,4}$	3.3	3.3	$J_{3',4'}$	3.4	
$J_{4,5}$	1.5	1.2	$J_{4',5'}$	1.5	
$J_{1,5}$	0.8	0.8	$J_{1',5'}$	0.8	
$J_{2,4}$	0.5	0.5	$J_{2',4'}$	0.5	
$J_{3,5}$	0.6	0.5	$J_{3',5'}$	0.5	
Compound 2					
H-1	5.36	4.67	H-1'	5.12	H-1'' 5.06
H-2	3.84	3.51	H-2'	3.78	H-2'' 3.75
H-3	4.07	3.81	H-3'	4.04	H-3'' 3.94
H-4	4.47	4.43	H-4'	4.47	H-4'' 4.33
H-5	4.71	4.37	H-5'	5.05	H-5'' 5.05
$J_{1,2}$	3.8	7.7	$J_{1',2'}$	4.0	$J_{1'',2''}$ 4.0
$J_{2,3}$	10.5	10.5	$J_{2',3'}$	10.7	$J_{2'',3''}$ 10.7
$J_{3,4}$	3.4	3.4	$J_{3',4'}$	3.4	$J_{3'',4''}$ 3.4
$J_{4,5}$	1.8	1.2	$J_{4',5'}$	1.5	$J_{4'',5''}$ 1.5

^a Long-range coupling constants have not been resolved.

and/or 0.3 Hz, except for the resonances of H-5 where changes of 0.17–0.22 p.p.m. were detected.

Based on the integrated intensities of the H-1 α and H-1 β resonances, the α,β -ratio was determined as 34:66. The $J_{1,2}$ values accorded with 4C_1 conformations of the pyranose units. Long-range couplings between rings protons in **1** were in the range 0.5–0.8 Hz; lower values were due to *gauche* (not *W*) arrangement of bonded atoms in the pyranose unit.

The ${}^{13}\text{C}$ data for **1** and **2** are given in Table II. The chemical shifts are within 1 p.p.m. of those for the Na^+ and Ca^{2+} forms, except for the C-5 and C-6 resonances where differences of 1.5–1.8 and/or 3.0–3.8 p.p.m. were detected.

*Experimental ${}^3J_{\text{C,H}}$ and *n.O.e.* data.* — In order to determine the conformations of the glycosidic bonds in **1** and **2**, the values of ${}^3J_{\text{C,H}}$ across the glycosidic linkages were measured at different temperatures (Table III).

TABLE II

${}^{13}\text{C}$ Chemical shifts (δ in p.p.m.) for solutions of **1** and **2** in D_2O at 25° (referenced to internal acetone, 30 p.p.m.)

Atom	α	β				
<i>Compound 1</i>						
C-1	92.00	96.09	C-1'	99.79		
C-2	67.50	70.77	C-2'	67.60		
C-3	62.60	71.27	C-3'	68.45		
C-4	78.12	77.32	C-4'	69.70		
C-5	69.12	72.56	C-5'	70.68		
C-6	171.75	170.87	C-6'	172.50		
<i>Compound 2</i>						
C-1	92.06	96.05	C-1'	99.58 ^a	C-1''	99.62 ^a
C-2	67.65	70.87	C-2'	67.65	C-2''	67.65
C-3	67.65	71.38	C-3'	67.91	C-3''	68.54
C-4	78.22	77.40	C-4'	77.94	C-4''	69.77
C-5	69.35	72.86	C-5'	70.09	C-5''	70.76
C-6	171.50	172.75	C-6'	172.32	C-6''	172.32

^a Chemical shifts may be reversed.

TABLE III

Experimental J^b and J^w values (Hz) for solutions of **1** (at 25° and 50°), and **2** (at 25°) in D_2O

Coupling constant	1 25°	1 50°	2 25°
J^b	3.7	3.7	3.7
J^w	4.9	5.0	5.1
$J^{b'}$			3.8
$J^{w'}$			5.1

For **1**, the J^{ϕ} ($J_{\text{H-1',C-4}}$) and J^{ψ} ($J_{\text{H-4,C-1'}}$) values were 3.7 and/or 4.9 Hz (25°) and 5.0 Hz (50°), respectively. For **2** comparable values of 3.7 (J^{ϕ}), 3.8 ($J_{\text{H-1',C-4}}$) and 5.1 Hz (both J^{ψ} and $J_{\text{H-4,C-1'}}$) were observed. Thus the inter-glycosidic couplings did not change significantly with temperature and were the same (within experimental error) for **1** and **2**. The corresponding dihedral angles ϕ^{H} and ψ^{H} , based on the relationship²¹ between $^3J_{\text{C,H}}$ and dihedral angles, were $\sim 40^\circ$ and/or $\sim 20^\circ$, respectively. However, owing to the degeneracy of the Karplus-type relationship, other values of both dihedral angles agreed with the experimental data.

For more precise characterisation of the conformation of the glycosidic bond, n.O.e. values were determined (Table IV). Changes in the intensities of the signals for **1** on saturation of H-1' were observed at both temperatures for H-4 β (9%), H-4 α (6%), and H-2' (24%). Similarly, simultaneous saturation of H-4 α and H-4 β caused a 19% enhancement of the signal for H-1' at 25° and 20% at 50°; a three-spin effect was observed on the signal for H-2' (−1%). Other enhancements at 25° and 50° were observed for the signals of H-3 α (6 and 6%), H-3 β (7 and 8%), H-5 α (5 and 5%), and H-5 β (5 and 5%). N.O.e.'s were detected also on saturation of H-5' for the signals of H-2 α (2 and 2%), H-2 β (4 and 4%), H-3' (10 and 11%), and H-4' (15 and 15%).

For **2** (data not shown), on saturation of both H-4 α and H-4 β , the enhancement of the signal for H-1' was 18%. The signals for H-1'' and H-5' overlapped and the sum of the n.O.e.'s was 21%. Saturation of H-1' caused a change of intensity of the signal for H-4 β (9%), and the sum of the n.O.e.'s for the signals of H-4 α and H-4' was 23%. Irradiation of H-5' caused a 2 and 5% increase in the intensities of the signals for H-2 α and H-2 β , respectively. Although analysis of n.O.e. data for **2** was not as straight-

TABLE IV

Experimental n.O.e. values (%) in (**1**) on pre-irradiation of H-1', H-4 β and H-4 α , and H-5' in aqueous solutions

Resonance observed	Proton saturated					
	H-1'		H-4 β + H-4 α		H-5'	
	25°	50°	25°	50°	25°	50°
H-1'			19	20		
H-2'	24	24	−1	−1		
H-3'					10	11
H-4'					15	15
H-2 α					2	2
H-2 β					4	4
H-3 α			6	6		
H-3 β			7	8		
H-4 α	6	6				
H-4 β	9	9				
H-5 α			5	5		
H-5 β			5	5		

forward as for **1** due to signal overlap, the magnitudes of n.O.e. effects that could be analysed were comparable to those of **1**.

Molecular mechanics calculations. — The coupling constants and n.O.e. effects are time-averaged and may not be correlated directly with the geometry of interconverting conformers. The experimental values should be compared with those calculated theoretically, including optimisation of the geometry and determination of conformer populations. The MM2CARB method has been used to minimise energy as a function of the geometrical parameters in order to determine the geometry and populations of conformers.

A relaxed (ϕ, ψ) map, computed as a function of ϕ and ψ in steps of 30° , is shown in Fig. 1. Four minima (1–4) were found on the energy surface, with ϕ^H and ψ^H values of $(-33, 29)$, $(-55, -34)$, $(-65, -80)$, and $(-54, 150)$ (Table V). The most stable conformers were **1** and **2**, with a difference in relative energies of 0.13 kJ.mol^{-1} (6.45 kJ.mol^{-1} for **3** and $16.41 \text{ kJ.mol}^{-1}$ for **4**). Dihedral angles (ω) between O-5 and C-6=O indicate that these oxygens are approximately antiperiplanar, as found in a previous study⁷ and independent of the conformation of the glycosidic bond. Computed $^3J_{C,H}$ values for conformers **1** and **2** are comparable with experimental values, but those for conformers **3** and **4** differ considerably.

For analysis of the stereochemistry of galacturono-oligo- and -poly-saccharides in solution, knowledge of the geometry of the glycosidic bond is crucial. The values of ϕ^H and ψ^H for conformer **1** indicate that two-fold helices could be formed, whereas those for conformer **2** agree with a right-handed three-fold arrangement.

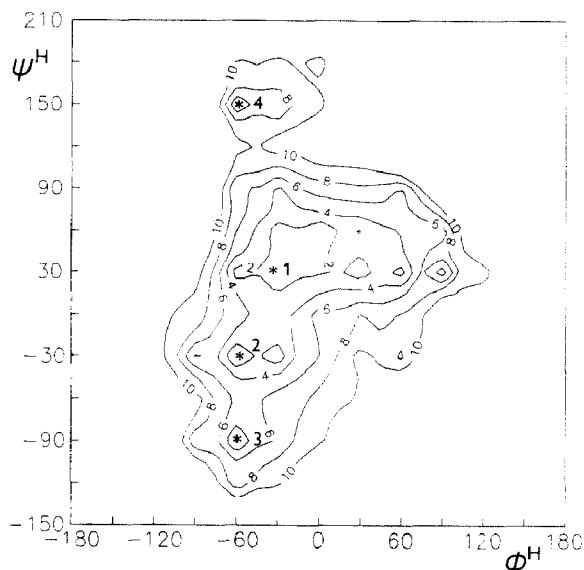


Fig. 1 Relaxed (ϕ, ψ) conformational map for **1** computed using the MM2CARB method as a function of ϕ and ψ in steps of 30° . Denoted minima 1–4 (asteriks) have the geometry of the glycosidic bond prior to optimisation of ϕ^H and ψ^H : $(-30, 30)$, $(-60, -30)$, $(-60, -90)$, and $(-60, 150)$.

TABLE V

MM2CARB-calculated energies ΔE (kJ.mol⁻¹), selected dihedral angles (°), and J^ϕ and J^ψ values (Hz) for the optimised conformers of **1** in the isolated state

Parameter	Conformer			
	1	2	3	4
ΔE	0	0.13	6.45	16.41
ϕ^H	-33	-55	-65	-54
ψ^H	29	-34	-80	150
ω	157	-169	162	152
J^ϕ	4.0	2.2	1.3	2.2
J^ψ	4.4	4.0	0.6	6.8

The abundances of the conformers, computed using a continuum model for evaluation of the effect of the solvent¹⁹, are listed in Table VI. Unlike the isolated state, where the two conformers have comparable abundances, the population changed in favour of conformer 2 in solution. The difference in populations decreases with an increase of temperature and with a decrease of the dielectric constant of the solvent. However, conformer 2 is present almost exclusively and conformers 3 and 4 have negligible abundance. The geometry of the most populated conformer is close to that (-47, -23) found for pectic acid in the solid state⁷. The stabilisation of conformer 2 in solution is probably due to the different values of dipole moments. The dipole moments for conformers 1 and 2 are 5.38 and 7.20 D, respectively. These values cause different solvation energies; for conformers 2 and 1, dipolar interactions were -13.81 and -6.49 kJ.mol⁻¹, respectively. Thus, MM2CARB calculations with evaluation of the solvent effect showed that, in solution, the conformers with glycosidic bond geometry (ϕ^H -55, ψ^H -34), corresponding to a right-handed three-fold helix, were favoured. In order to confirm this trend, the n.O.e. effects were calculated based on the geometry of conformer 2 (Table VII). When H-1' was saturated, the computed n.O.e. effect on the signals of H-4 α and H-4 β was 18%, and 20% on that for H-2'. Theoretical values comparable with those found experimentally were also found on saturation of H-4 with the following enhancements in signals H-1', 25%; H-3 α , H-3 β , 16%; and H-5 α , H-5 β , 5%. Similarly, when H-5' was saturated, the changes in intensities of the signals calculated for H-2 α and H-2 β were 4% (experimental 6%), and for H-3' and H-4', 7% and 12%, respectively (experimental 10 and 15%).

For comparison, n.O.e. effects based on the geometry of conformer 1 were calculated. Computed enhancements (not shown) for the resonances of H-1' and H-4 showed values that were different from those listed in Table VII. For instance, on saturation of H-1', the change of intensity of the signal for H-4 was 7%; on saturation of H-4, the enhancement of the signal for H-1' was 32%. Significant differences were obtained for the signals of H-2 α and H-2 β when H-5' was irradiated. The computed n.O.e. based on the geometry of conformer 1 was 32%, compared to 4% based on the geometry of conformer 2 (experimental 6%). This result reflects different inter-proton

TABLE VI

MM2CARB-calculated molar fractions (%) and averaged coupling constants $\langle J^{\phi} \rangle$ and $\langle J^{\psi} \rangle$ (Hz) for the optimised conformers 1–4 of **1** for the isolated state and for solutions in water and methyl sulfoxide

Solution	Conformer				$\langle J^{\phi} \rangle$	$\langle J^{\psi} \rangle$
	1	2	3	4		
Isolated state	49	47	4	0	3.0	4.2
Water 25°	5	94	1	0	2.3	4.0
50°	7	91	2	0	2.3	4.0
70°	9	89	2	0	2.3	4.0
Methyl sulfoxide 25°	20	78	2	0	2.5	4.0

TABLE VII

Calculated n.O.e. values^a (%) for **1** based on the geometry of conformer 2 on pre-irradiation of H-1', H-4 β and H-4 α , and H-5' in aqueous solutions at 25°

Resonance observed	Proton saturated		
	H-1'	H-4 β + H-4 α	H-5'
H-1'		25	
H-2'	20		
H-3'			7
H-4'			12
H-2 α + H-2 β			4
H-3 α + H-3 β		16	
H-4 α + H-4 β	18		
H-5 α + H-5 β		5	

^a For protons on the reducing unit, the sum of n.O.e. enhancements for α and β anomers was calculated.

distances obtained from the MM2CARB calculations. In conformer 1, the distance between H-5' and H-2 is 219 pm; in conformer 2, the distance is 283 pm. The presence of conformer 2 in solution also supports the magnitudes of J^{ϕ} and J^{ψ} , which differ, thereby reflecting the different values of ϕ^H and ψ^H in conformer 2, whereas the angles have comparable values for conformer 1.

Although the MM2CARB method with a continuum model for evaluation of the effect of the solvent gives only approximate results, based on the agreement between experimental and theoretical values, it is inferred that the geometry of conformer 2 is close to that of the glycosidic bond of pectin acid oligosaccharides in solution.

Thus, the conformations of the glycosidic bonds in **1** and **2** are approximately the same. The magnitudes of ϕ^H and ψ^H (–55, –34) suggest that a right-handed three-fold helical arrangement may be formed in pectic acid oligosaccharides in solution. The populations of the conformers do not change considerably with temperature, as reflected by the constant values of the experimental n.m.r. parameters. Moreover, in the isolated state, two conformers showed comparable populations, and changes in the

environment favoured conformer 2. This fact indicates the considerable effect of the environment on the conformation of the glycosidic bond, even in a relatively rigid glycosidic linkage such as the diaxial type.

REFERENCES

- 1 E. R. Morris and S. A. Frangou, in D. H. Northcote (Ed.), *Techniques in Carbohydrate Metabolism*, Elsevier Applied Science, London, 1981. pp. 1–51.
- 2 L. Alagna, T. Prosperi, and A. A. G. Tomlinson, *J. Phys. Chem.*, 90 (1986) 6853–6857.
- 3 K. Wuhrmann and W. Pilnik, *Experientia*, 1 (1945) 330–332.
- 4 K. J. Palmer and M. B. Hartzog, *J. Am. Chem. Soc.*, 67 (1945) 2122–2127.
- 5 D. A. Rees and A. W. Wight, *J. Chem. Soc., B.*, (1971) 1366–1372.
- 6 B. K. Sathyanarayana and V. S. R. Rao, *Curr. Sci.*, 42 (1973) 773–775.
- 7 M. D. Walkinshaw and S. Arnott, *J. Mol. Biol.*, 153 (1981) 1055–1073.
- 8 A. Cesaro, A. Ciana, F. Delben, G. Manzini, and S. Paoletti, *Biopolymers*, 21 (1982) 431–449.
- 9 J. F. Thibault and M. Rinaudo, in M. L. Fishman and J. J. Jen (Eds.), *ACS Symp. Ser. No. 310*, (1986) 61–72.
- 10 S. Bystricky, A. Malovikova, and T. Sticzay, *Carbohydr. Polym.*, in press.
- 11 R. Kohn, *Carbohydr. Res.*, 20 (1971) 351–356.
- 12 R. Kohn, K. Heinrichová, and A. Malovíková, *Collect. Czech. Chem. Commun.*, 48 (1983) 1922–1935.
- 13 M. Hricovini and T. Liptaj, *Magn. Reson. Chem.*, 27 (1989) 1052–1056.
- 14 M. Hricovini, I. Tvaroška, D. Uhrin, and G. Batta, *J. Carbohydr. Chem.*, 8 (1989) 389–394.
- 15 D. Neuhaus, *J. Magn. Reson.*, 53 (1983) 109–114.
- 16 N. L. Allinger, *J. Am. Chem. Soc.*, 99 (1977) 8127–8134.
- 17 G. A. Jeffrey and R. Taylor, *J. Comput. Chem.*, 1 (1980) 99–109.
- 18 I. Tvaroška and J. Gajdoš, *Chem. Pap.*, 41 (1987) 485–500.
- 19 I. Tvaroška and T. Kožár, *J. Am. Chem. Soc.*, 102 (1980) 6929–6936.
- 20 M. Rinaudo, G. Ravanat, and M. Vincendon, *Macromol. Chem.*, 181 (1980) 1059–1070.
- 21 I. Tvarorška, M. Hricovini, and E. Petráková, *Carbohydr. Res.*, 189 (1989) 359–362.